

# Cross-Modal Attention Consistency for Video-Audio Unsupervised Learning

Shaobo Min<sup>1\*</sup>, Qi Dai<sup>2</sup>, Hongtao Xie<sup>1†</sup>, Chuang Gan<sup>3</sup>, Yongdong Zhang<sup>1</sup>, and Jingdong Wang<sup>2</sup>

<sup>1</sup>University of Science and Technology of China

<sup>2</sup>Microsoft Research Asia

<sup>3</sup>MIT-IBM Watson AI Lab

## Abstract

Cross-modal correlation provides an inherent supervision for video unsupervised representation learning. Existing methods focus on distinguishing different video clips by visual and audio representations. We human visual perception could attend to regions where sounds are made, and our auditory perception could also ground their frequencies of sounding objects, which we call bidirectional local correspondence. Such supervision is intuitive but not well explored in the contrastive learning framework. This paper introduces a pretext task, Cross-Modal Attention Consistency (CMAC), for exploring the bidirectional local correspondence property. The CMAC approach aims to align the regional attention generated purely from the visual signal with the target attention generated under the guidance of acoustic signal, and do a similar alignment for frequency grounding on the acoustic attention. Accompanied by a remoulded cross-modal contrastive loss where we consider additional within-modal interactions, the CMAC approach works effectively for enforcing the bidirectional alignment. Extensive experiments on six downstream benchmarks demonstrate that CMAC can improve the state-of-the-art performance on both visual and audio modalities.

## 1. Introduction

Unsupervised image representation learning [47, 37, 15, 19, 7] has attracted great attention recently, which attempts to learn useful knowledge from massive unlabeled data and transfer to various downstream tasks. Nevertheless, the efforts in video counterpart are still inapparent, though the multi-modal nature is particularly suitable for unsupervised learning by providing intensive coherence and variation information. This paper focuses on the Video-Audio Unsupervised Learning task [25, 30, 38, 25], which aims at

exploring cross-modal clues to simultaneously learn visual and audio representations from massive unlabeled videos.

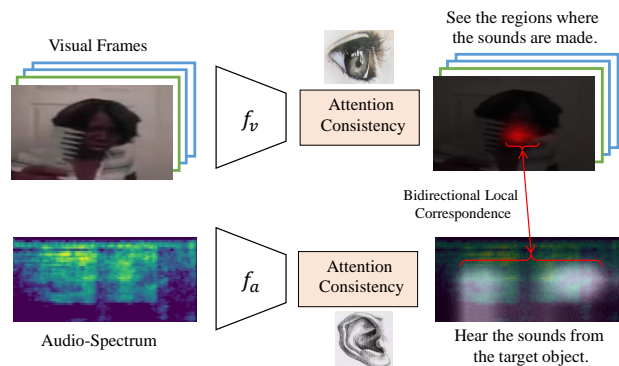


Figure 1. CMAC expects the visual encoder to focus on the regions where sounds are made and the audio encoder to focus on sounds from the interested objects.

A general technique [25, 30] in the literature is to leverage the intrinsic correspondence between visual frames and audio waves by determining whether they are from the same video instance. With recent advances of contrastive learning [48, 19], these approaches make positive (negative) video-audio pairs similar (dissimilar). Based on this paradigm, AVTS [25] designs a harder synchronization supervision, which defines positive visual-audio pairs only when they are from the identical clip of a video. In addition to cross-modal discrimination, AVID [30] considers within-modal discrimination, which simultaneously explores the relationship between visual-audio, visual-visual, and audio-audio pairs. Recently, GDT [38] develops a unified visual-audio contrastive framework by exploring more comprehensive data augmentations and modality relationship.

Despite the impressive performance of the above methods, their pretext supervisions only consider the instance level relationship between global modality representations, *e.g.* the aggregated spatio-temporal features and audio spectrogram features [1, 38]. This inevitably discards fine-grained local clues, *i.e.* the relation between each spatio-temporal region and foreground sound frequency. In the

\*Work was done during internship at Microsoft.

†Corresponding author.

human sensory system, our visual perception is sensitive to the spatial regions where sounds are made, and vice versa our auditory perception is sensitive to the sound frequencies belonging to foreground objects. This phenomenon, called *bidirectional local correspondence*, is natural and intuitive to associate spatio-temporal visual clues with acoustic frequencies. Some early works [2, 35, 34] study the global alignment between modalities for representation learning, while ignoring such local relation. One recent exploration [23] considers it in image feature learning via co-clustering. However, their method has not been validated in the challenging large-scale video unsupervised learning task.

In this paper, we propose a novel pretext task, namely Cross-Modal Attention Consistency (CMAC), for exploring the *bidirectional local correspondence* property between visual and acoustic signals. The core insight is to make the visual encoder attend to regions where sounds are made and the audio encoder attend to sound frequencies from interested objects, as shown in Fig. 1. To achieve the goal, CMAC proposes to align the *regional attention* generated purely from the visual signal with the *target attention* generated under the guidance of acoustic signal, and do a similar alignment for frequency grounding on the acoustic attention. Compared with traditional cross-modal contrastive manner [1, 38], CMAC provides a novel mechanism that considers bidirectional local correspondence between spatio-temporal visual clues and audio-spectrogram signals via attention consistency.

Specifically, to produce the target cross-modal attention without human annotations, we devise a pyramid attention mechanism. CMAC first dynamically learns a set of adaptive filters (kernels) in each modality. To generate target attention for one modality (*e.g.* visual), the learned filters from the other modality (*i.e.* audio-induced) are utilized to perform filtering on its representations (*i.e.* visual). The predicted audio-guided visual attention map thus indicates the spatio-temporal regions that are most related to audio signals, and vice versa for the visual-guided audio attention map. With the learned cross-modal attention maps as supervision, CMAC then preserves the attention consistency between them and the single-modality induced attention maps.

The proposed attention consistency works effectively in accompany with a remoulded contrastive loss, where additional within-modal information is considered. Different from AVID [30], we only involve within-modal negative samples from previous batch data, thereby without extra memory cost for resampling within-modal positive samples for the current batch. This simple yet effective modification successfully boosts the performance. Experiments on various downstream tasks including action recognition, video retrieval, and audio classification show that CMAC can improve the state-of-the-art results.

The contributions of this paper are three-fold: (1) We

show that the *bidirectional local correspondence* is effective in cross-modal representation learning; (2) A novel pretext task namely Cross-Modal Attention Consistency (CMAC) is introduced for unsupervised learning; (3) New state-of-the-art results are achieved by CMAC on various downstream benchmarks.

## 2. Related Works

Unsupervised representation learning targets at learning good data representations in an unsupervised manner.

**Unsupervised learning from images.** Due to unavailable human annotation, existing methods focus on designing pretext tasks [10, 47, 37, 15] to learn good data representations. For example, a seminal work [11] augments each image into several transformations and regards each image as an exemplar, thus a traditional classification task can be defined as recognizing image transformations into their exemplar category. Besides, CFN [32] designs a jigsaw puzzle task by predicting orders of different patches from the same image, and RotNet [15] predicts the rotation angles of an image. These proxy tasks aim to understand some low-level image concepts, such as rotation invariance and spatial relationship among image patches. Recently, contrastive loss [17, 48, 33, 22, 52, 21, 6, 16] has attracted great attention, which makes different transformations from the same image attract and those from different images repel. Compared to fixed prototypes in exemplar methods, the contrastive loss can vary on-the-fly training. Two representative methods are MoCo [19] and SimCLR [7]. MoCo designs a dynamic dictionary with a moving-averaged encoder to store a large-scale and consistent instance representation set, and SimCLR explores the importance of projection head and comprehensive data augmentations in unsupervised learning.

**Cross-modal unsupervised learning.** Compared to images, videos are more commonly seen and contain a rich variety of modalities, *e.g.* visual, audio, and speech signals. The correlation between different modalities is a natural supervision that has attracted increasing interest [9]. Some works [45, 29, 27, 31] leverage the speech as a weak supervision, and other works explore the audio self-supervision to boost visual localization [42], audio-visual source separation [18, 12, 13, 41], and representation learning [2, 34, 40, 3]. In this work, we focus on visual-audio unsupervised learning, which aims at jointly learning visual and audio representations in an unsupervised manner. A general paradigm is to detect whether the visual and audio signals are from the same video, which is commonly solved via cross-modal contrastive learning [25, 30, 38, 49]. AVTS [25] further employs the temporal synchronization by defining positive visual-audio pairs only when they are temporally synchronized, constraining the representations to understand the temporal content. In addition to the cross-modal learning, AVID [30] introduces the within-modal

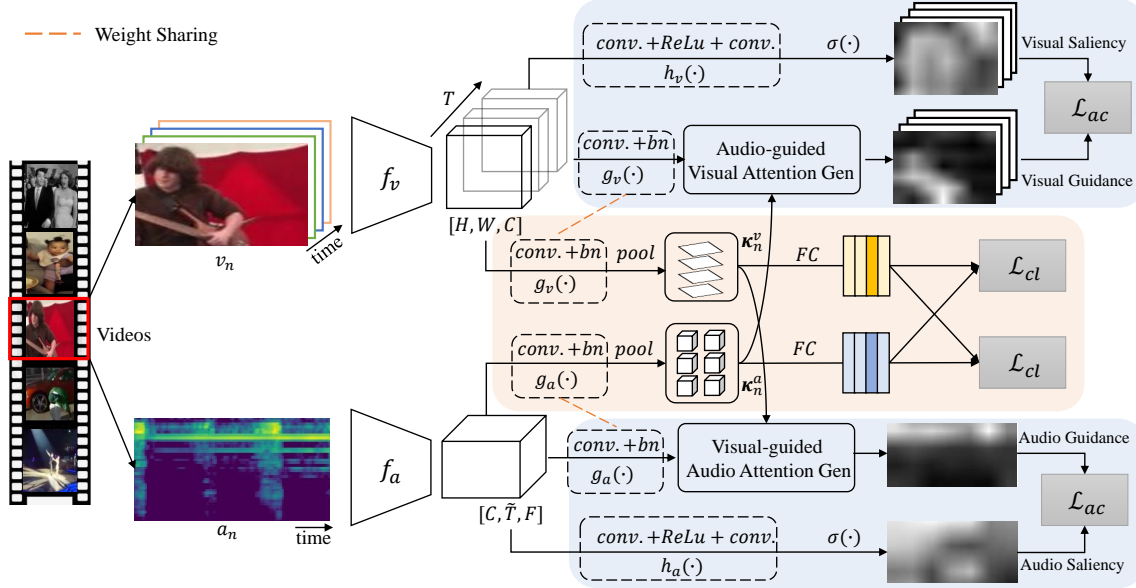


Figure 2. Overview of CMAC. We aim to align *regional attention* generated purely from the visual signal with *target attention* generated under the guidance of audio signal, and do the similar alignment for the audio counterpart. CMAC first produces filters for both modalities, and then generates cross-modal guided attention by searching the most matched patterns in one modality in terms of filters from the other modality. The guided attention is used to supervise the single-modal attention via attention consistency  $\mathcal{L}_{ac}$ . A remoulded contrastive loss  $\mathcal{L}_{cl}$  is leveraged to bridge the semantic gap between filters of two modalities by considering additional within-modal negative samples.

information via extra visual-visual and audio-audio contrastive learning, but it requires doubling the memory cost for both within- and cross-modal positive pairs. GDT [38] explores more comprehensive data augmentations and data pair constructions. Different from cross-modal contrastive learning, XDC [1] leverages unsupervised clustering in one modality to supervise representations of the other modality. AVSlowFast [49] proposes a visual-audio encode architecture that contains slow and fast visual pathways to explore knowledge at different temporal scales. Though above methods achieve promising results, they only consider cross-modal instance discrimination by distinguishing different clips, while ignoring the local correspondence between spatio-temporal regions and acoustic frequencies.

Notably, the visual-audio local correspondence has been partially studied in visual-audio localization [51, 41] and representation learning [23] methods. For example, DMC [23] treats the local features in image feature maps as a set of distinct components, and learns the visual and auditory subnets by co-clustering them. Though the learned visual features perform well in image classification on small datasets, however, this method has not been validated in the challenging unsupervised video pretraining task. In contrast to the clustering-based learning in DMC, in this paper we propose a novel attention-based method to explore the effectiveness of local correspondence in this challenging task, rather than learning exact localization between modalities.

### 3. Method

#### 3.1. Preliminaries

Suppose we have a set of videos  $\{\mathbf{x}\}$  consisting of a visual track (RGB frames) and an audio track (sound), the target of visual-audio unsupervised learning is to learn feature encodings  $f_v(\cdot)$  and  $f_a(\cdot)$  for both modalities that can well transfer to various downstream visual or audio tasks.

Formally, we define  $(\mathbf{v}_n, \mathbf{a}_n)$  as the encoded visual and audio representations of the  $n$ -th video, *i.e.*  $\mathbf{v}_n = f_v(\mathbf{x}_n)$ ,  $\mathbf{a}_n = f_a(\mathbf{x}_n)$ . A general paradigm is to detect synchronized pair of  $(\mathbf{v}, \mathbf{a})$  in a contrastive manner. When  $\mathbf{v}$  and  $\mathbf{a}$  are from the same location of one video, they are synchronized and identified as positive sample pair. When they are from different videos, they form a negative pair. By sampling massive positive and negative visual-audio pairs, the *noise-contrastive loss* [7, 48] can be formulated as:

$$\mathcal{L}_{nce}(\mathbf{v}, \mathbf{a}) = -\frac{1}{N} \sum_{n=1}^N \log \frac{\text{sim}(\mathbf{v}_n, \mathbf{a}_n)}{\sum_m \text{sim}(\mathbf{v}_n, \mathbf{a}_m)}, \quad (1)$$

where  $\text{sim}(x, y) = e^{\langle x, y \rangle / \tau}$ , and  $\langle \cdot, \cdot \rangle_{\tau}$  is the cosine similarity divided by a temperature parameter  $\tau$ .  $N$  is the size of batch. When  $m \neq n$ ,  $\mathbf{a}_m$  is a negative sample. For simplicity, we omitted the visual and audio augmentations here. The final cross-modal contrastive loss becomes:

$$\mathcal{L}_{nce}(\mathbf{v}, \mathbf{a}) + \mathcal{L}_{nce}(\mathbf{a}, \mathbf{v}). \quad (2)$$

Eq. (2) indeed leverages the intrinsic synchronization between visual and audio signals as supervision, *i.e.*, detecting whether the input visual and audio representations are synchronized. However, in human perception mechanism, a more intuitive supervision is that our visual system usually focuses on the regions where sounds are made, and our auditory system focuses on the frequencies that belong to interested objects, called *bidirectional local correspondence*. To introduce such an important pretext supervision, we propose a novel Cross-Modal Attention Consistency framework, of which the illustration is shown in Fig. 2.

### 3.2. Cross-Modal Attention Consistency

The proposed Cross-Modal Attention Consistency (CMAC) aims to explore the bidirectional local correspondences between  $v$  and  $a$  to supervise the visual encoder  $f_v(\cdot)$  and audio encoder  $f_a(\cdot)$ . To achieve the goal, CMAC tackles two challenges: a) how to localize the crucial spatio-temporal regions and acoustic frequencies as supervisions, and b) how to constrain  $f_v(\cdot)$  and  $f_a(\cdot)$  to concentrate on the localized regions and frequencies.

Given a synchronized pair<sup>1</sup>  $v_n \in \mathbb{R}^{C \times T \times H \times W}$  and  $a_n \in \mathbb{R}^{C \times \tilde{T} \times F}$ , CMAC first estimates a set of adaptive filters (kernels) on visual and audio representations by

$$\kappa_n^v = \text{pool}(g_v(v_n)), \quad \kappa_n^a = \text{pool}(g_a(a_n)), \quad (3)$$

where  $g_v(\cdot)$  and  $g_a(\cdot)$  are two transformation functions implemented by *conv. + bn* operations.  $\kappa_n^v$  and  $\kappa_n^a$  are the produced filters for visual and audio modalities, respectively.  $\text{pool}(\cdot)$  is the pooling function that controls the kernel size of  $\kappa_n^v$  and  $\kappa_n^a$ . Here, we adopt the global average pooling for simplicity, which means  $\kappa_n^v \in \mathbb{R}^{C \times 1 \times 1 \times 1}$  and  $\kappa_n^a \in \mathbb{R}^{C \times 1 \times 1}$ . These filters provide the modality-specific essentials for capturing related contents in the other modality. With  $\kappa_n^v$  and  $\kappa_n^a$ , we leverage the attention mechanism to highlight the corresponding contents by devising a *pyramid correlation filtering* module for each modality.

**Pyramid Correlation Filtering.** To generate the target attention map for one modality, *e.g.* visual, we utilize the learned filters from the other modality, *i.e.* audio, to perform Pyramid Correlation Filtering (PCF) on its representations (*i.e.* visual). The core insight is to search the most matched patterns in one modality in terms of filters from the other modality. Consequently, the attention map  $s_n^v$  ( $s_n^a$ ) is calculated by convolving the filter  $\kappa_n^a$  ( $\kappa_n^v$ ) over the modality representation  $v_n$  ( $a_n$ ), which can be formulated as

$$s_n^v = \text{norm}(\kappa_n^a * g_v(v_n)), \quad s_n^a = \text{norm}(\kappa_n^v * g_a(a_n)), \quad (4)$$

where  $s_n^v \in \mathbb{R}^{T \times H \times W}$  is the audio-guided visual attention for  $v_n$ , and  $s_n^a \in \mathbb{R}^{\tilde{T} \times F}$  is the visual-guided audio attention

<sup>1</sup> $\{C, T, H, W\}$  denote channel, frame, height, and width respectively.  $\{\tilde{T}, F\}$  indicate the time and frequency.  $\tilde{T}$  is determined by window width of FFT and is generally different from  $T$ .

for  $a_n$ . Here  $g_v(\cdot)$  and  $g_a(\cdot)$  are shared with that in Eq. (3).  $*$  denotes the convolution operation. For instance,  $s_n^v$  measures the similarity response between  $\kappa_n^a$  and each local feature in  $v_n$ .  $\text{norm}(\cdot)$  maps the response map into  $[0, 1]$ , where the cosine-based normalization is used in this paper. The predicted audio-guided visual attention  $s_n^v$  indicates the spatio-temporal regions that are most related to the audio signals, *i.e.* regions where the sounds are made. Similarly,

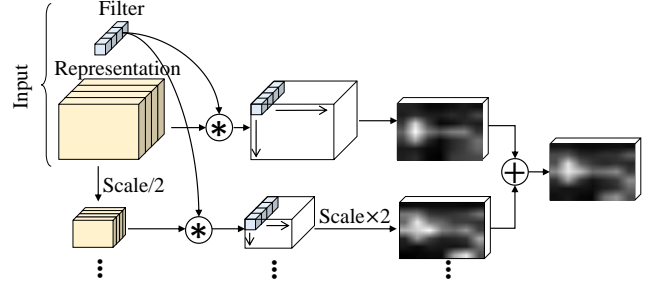


Figure 3. Pyramid Correlation Filtering (PCF). The inputs of PCF contain a representation and corresponding filters. PCF convolves filters over the representations at each position and obtains a response map. Notably, a pyramid scaling strategy is used to fuse the multi-scale responses.

the visual-guided audio attention  $s_n^a$  indicates the acoustic frequencies from the interested objects.

It is worth noting that we adopt a pyramid scaling strategy to obtain better attention clues. Since both  $s_n^v$  and  $s_n^a$  preserve the original scales of representations, we further downsample  $v_n$  and  $a_n$  to the half resolution and calculate the filter response again, as shown in Fig. 3. As a result, we fuse the response maps at different scales to generate the final attention map.

**Attention Consistency.** For exploring local corresponding patterns between  $v_n$  and  $a_n$ , the learned  $s_n^v$  and  $s_n^a$  can be regarded as pseudo labels that  $f_v(\cdot)$  and  $f_a(\cdot)$  should focus on. As illustrated in Fig. 2, CMAC first exploits two saliency detection heads to directly infer the within-modal attention maps  $\hat{s}_n^v, \hat{s}_n^a$  purely from  $v_n, a_n$  by:

$$\hat{s}_n^v = \sigma(h_v(v_n)), \quad \hat{s}_n^a = \sigma(h_a(a_n)), \quad (5)$$

where  $h_v(\cdot)$  and  $h_a(\cdot)$  are two convolution blocks for predicting the attention maps, and  $\sigma(\cdot)$  is the sigmoid function. The learned single-modality induced maps  $\hat{s}_n^v, \hat{s}_n^a$  imply the concentrations of the modality encoders  $f_v(\cdot), f_a(\cdot)$ . Accordingly, the attention consistency can be preserved by aligning them with the previous cross-modal attention maps  $s_n^v, s_n^a$  as follows:

$$\mathcal{L}_{ac}(s_n^v, \hat{s}_n^v) = \|s_n^v - \hat{s}_n^v\|_2^2, \quad \mathcal{L}_{ac}(s_n^a, \hat{s}_n^a) = \|s_n^a - \hat{s}_n^a\|_2^2. \quad (6)$$

**Contrastive Learning.** In the above Pyramid Correlation Filtering, directly performing the cross-modal correlation

filtering would lead to degradation as the filter and representation are from different modalities with a serious statistical gap. To this end, we leverage the contrastive learning to bridge the modality gap between  $\kappa_n^a$ ,  $\kappa_n^v$  and  $v_n$ ,  $a_n$ . Specifically, both  $\kappa_n^v$  and  $\kappa_n^a$  are projected into joint embedding space via FC projection heads. A cross-modal contrastive loss  $\mathcal{L}_{cl}$  is then leveraged to align them with the instance discrimination supervision, so that they can learn cross-modal knowledge:

$$\mathcal{L}_{cl}(\kappa_n^v, \kappa_n^a) = -\log \frac{\text{sim}(\kappa_n^v, \kappa_n^a)}{\sum_m \text{sim}(\kappa_n^v, \kappa_m^a) + \sum_{m \neq n} \text{sim}(\kappa_n^v, \kappa_m^v)}. \quad (7)$$

Here we omit the projection heads for simplicity.  $\mathcal{L}_{cl}$  is a variant of contrastive loss, where the main difference between  $\mathcal{L}_{cl}$  and  $\mathcal{L}_{nce}$  is that we include within-modal negative pairs  $(\kappa_n^v, \kappa_m^v)$  in Eq. (7) to introduce within-modal discrimination knowledge, which is ignored by most of the existing methods [25, 49, 38] as in Eq. (1). AVID [30] also considers the within-modal knowledge by adding  $\mathcal{L}_{nce}(v_{n1}, v_{n2})$  and  $\mathcal{L}_{nce}(a_{n1}, a_{n2})$  to Eq. (1), which, however, requires saving two clips for  $n$ -th video in a mini-batch as positive pairs. In contrast, our simple yet effective modification requires no extra positive samples and no additional memory overhead.

Notably, the contrastive learning of  $\mathcal{L}_{cl}$  has two main effects on CMAC: a) introducing within- and cross-modal instance discrimination knowledge which has been proved crucial and fundamental for  $f_v(\cdot)$  and  $f_a(\cdot)$  [25, 38]; and b) bridging the modality gap between  $\kappa_n^a$ ,  $\kappa_n^v$  and  $v_n$ ,  $a_n$ .

**Optimization.** Finally, the overall objective function of CMAC becomes:

$$\mathcal{L}_{all} = \mathcal{L}_{cl}(\kappa_n^v, \kappa_n^a) + \mathcal{L}_{cl}(\kappa_n^a, \kappa_n^v) + \lambda[\mathcal{L}_{ac}(s_n^v, \hat{s}_n^v) + \mathcal{L}_{ac}(s_n^a, \hat{s}_n^a)], \quad (8)$$

where  $\lambda$  is a hyper-parameter to balance contrastive loss and attention consistency loss.

## 4. Experiments

The experiments are conducted by transferring pre-trained representations of Cross-Modal Attention Consistency (CMAC) to various downstream tasks, as well as several ablation studies. For additional experimental results, please refer to the supplementary material.

### 4.1. Pretraining Setting

For pretraining, the standard visual-audio dataset of Kinetics-400 [24] is used, which contains 240K videos of about 10 seconds. After filtering out bad instances, *e.g.* no audio signals, about 220K videos are used for pretraining. The results on the large-scale AudioSet [14] are provided in supplementary material.

CMAC aims to learn a visual encoder  $f_v(\cdot)$  and an audio encoder  $f_a(\cdot)$  in unsupervised manner. R(2+1)D-18 [46] is used as  $f_v(\cdot)$ , and ResNet-9 [20] is used as  $f_a(\cdot)$ . For each video instance in a batch, we randomly sample 1-second clip and produce visual modality data and audio modality data. This makes our positive visual-audio pairs always synchronous from the same video and negative visual-audio pairs from different videos, which is different from [25, 38]. The augmentation for the visual modality contains random cropping  $128 \times 128$  and random horizontal flipping. The augmentation for audio modality employs log mel filtering with 257 bank filters, time warping, random frequency masking, and random time masking in SpecAugment [36]. The contrastive learning in CMAC adopts MoCo [19] with default settings, *e.g.*,  $\tau = 0.07$ , memory bank size as 15000, and momentum update parameter as 0.999. The channels of cross-modal filters and contrastive head are 512 and 256, respectively. For optimization, we use SGD optimizer with  $lr = 0.01$ , weight decay  $1e - 5$ , momentum 0.9, and mini-batch size 128 on 8 V100 GPUs. A gradual warp-up schedule is utilized for the first 10 epochs.

### 4.2. Downstream Setting

**Video Action Recognition.** We evaluate the visual representations from  $f_v(\cdot)$  on two widely-used benchmarks, UCF101 [43] and HMDB51 [26]. UCF101 contains ~13K videos of 101 action classes, and HMDB51 contains ~7K videos of 51 activity classes. During training, we randomly sample 10 clips of 32 frames for each video. For visual augmentation, we follow [38] and use random cropping, color jitter, and random horizontal flipping. For optimization, we use SGD with  $lr = 0.005$ , weight decay as  $5e - 3$ , and momentum as 0.9. We use a mini-batch of 16 and train for 12 epochs. During testing, we uniformly sample 10 clips for each video, average their softmax scores, and report the class with the highest score. The averaged top-1 accuracies across three split folds are reported for both UCF101 and HMDB51.

**Video Action Retrieval.** For the video retrieval task, we report the recall metric of 1, 5, 10 samples for split-1 of UCF101 and HMDB51 datasets, following the protocol in [50]. The features are directly extracted from the pretrained models without finetuning. For each video, we uniformly sample 10 clips and average their pooled features after the last residual block. We use samples from the validation set to query samples in the training set according to K-NN strategy and cosine distance.

**Audio Classification.** We evaluate the audio representation from  $f_a(\cdot)$  on ESC50 [39], DCASE2013 [44] and DCASE2014 [44] benchmarks by quickly training a linear classifier. ESC50 contains 2K audio clips from 50 different classes. DCASE2013 and DCASE2014 contain 100 training clips from 10 different classes. For each audio in



Table 1. Evaluation of Attention Consistency (Att. Cons.) and Contrastive Loss (Contr. Loss) in CMAC.

Method	Att. Cons.	Contr. Loss	UCF101	HMDB51
Scratch	✗	✗	73.2	23.7
Single Modality	✗	✓	82.5	47.3
CMAC w/o $\mathcal{L}_{cl}$	✓	✗	76.4	25.1
CMAC w/o $\mathcal{L}_{ac}$	✗	✓	85.5	56.4
CMAC	✓	✓	87.2	57.8

ESC50, we sample 10 clips of 2-second length for training, and average the predicted scores of sampled 10 clips for testing. For DCASE2013 and DCASE2014, we extract 60 clips of 1-second length for training and testing.

### 4.3. Understanding Cross-Modal Attention Consistency

We present four ablation studies to evaluate each component of CMAC. For efficient validation, these experiments are conducted by pretraining on Kinetics with 50 epochs, batch size of 64, and finetuning on split-1 of UCF101 and HMDB51 without color jitter augmentation.

#### 4.3.1 Effect of each Component in CMAC

CMAC essentially learns two kinds of knowledge, *i.e.*, cross-modal attention consistency and instance discrimination, with  $\mathcal{L}_{ac}$  and  $\mathcal{L}_{cl}$ , respectively. Here, we evaluate their effects in Table 1. We begin with the baseline of CMAC w/o  $\mathcal{L}_{cl}$ , since  $\mathcal{L}_{cl}$  is also crucial to the attention consistency knowledge by bridging the modality gap between filters. Note that removing both  $\mathcal{L}_{cl}$  and  $\mathcal{L}_{ac}$  will invalidate the pretraining (*i.e.* from Scratch). The results show that, without bridging the modality gap between filters, CMAC can hardly produce reasonable guided attentions for consistency preserving, thus leading to similar results to training from scratch. Then, we add  $\mathcal{L}_{cl}$  but remove  $\mathcal{L}_{ac}$ , which indicates that only instance discrimination knowledge is introduced. This improves the performance from 76.4% to 85.5% on UCF101, demonstrating the great importance of cross-modal contrastive learning. We also list the inferior results of single modality contrastive learning for comparison. Finally, with both  $\mathcal{L}_{cl}$  and  $\mathcal{L}_{ac}$ , the result is further increased from 85.5% to 87.2%, which proves the effectiveness and complementarity of attention consistency knowledge. In summary, the bidirectional local correspondence between visual and audio signals can obviously benefit the fine-grained video content understanding.

#### 4.3.2 Analysis of $\lambda$

We evaluate the effects of cross-modal attention consistency  $\mathcal{L}_{ac}$  by varying  $\lambda$  in Eq. (8). From Fig. 4, it can be observed that, when  $\lambda$  increases from 0 to 1.5, the performance of CMAC is stably improved from 85.5% to 87.2%

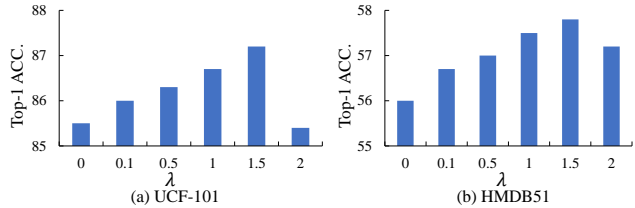


Figure 4. Evaluation for different  $\lambda$  on UCF-101 and HMDB-51.

Table 2. Evaluation of choices in the pyramid correlation filtering.

	<i>norm.</i>	Scale	UCF101	HMDB51
PCF	None	1	85.8	57.0
	softmax	1	86.6	57.4
	cosine	1	87.0	57.6
		2	87.2	57.9
		3	86.9	57.8

on UCF101. This proves that adding attention consistency for both visual and audio modalities can boost the encoders to understand visual content, thereby obtaining better downstream evaluation. When  $\lambda$  is larger than 1.5, the performance drops. The reason may be that the localized spatio-temporal regions from audio kernels are not accurate enough. Thus imposing strong cross-modal attention consistency may suffer from noisy attention maps. Finally, we set  $\lambda = 1.5$  in the following experiments.

#### 4.3.3 Analysis of Pyramid Correlation Filtering

In terms of pyramid correlation filtering (PCF), we conduct several experiments to search for a suitable architecture for generating the guided attention maps, as demonstrated in Table 2. The baseline is that PCF uses no normalization for convolution operation ( $*$ ) in Eq. (4) and no multi-scale fusion. Thus, the guided attention maps produced by filters and representations may be out of range  $[0, 1]$ , which makes the attention gradient unstable. Then, we add Softmax operation to normalize the response map, which brings gains on both datasets, *e.g.* 0.8% improvement on UCF101. However, the Softmax operation tends to suppress most of the regions, which slows the training at the beginning stage. To this end, we further replace the Softmax with a cosine normalization for  $*$ , which brings obvious improvements. Next, with the cosine normalization, we evaluate the effects of fusing multi-scale attention maps. We observe that fusing two-scale attention maps obtains the best attention guidance for both datasets. The reason may be that, due to limited memory resources, the spatial resolution of the final visual representation of  $f_v(\cdot)$  has been reduced from  $128 \times 128$  to  $8 \times 8$ , indicating that a two-scale fusion is enough.

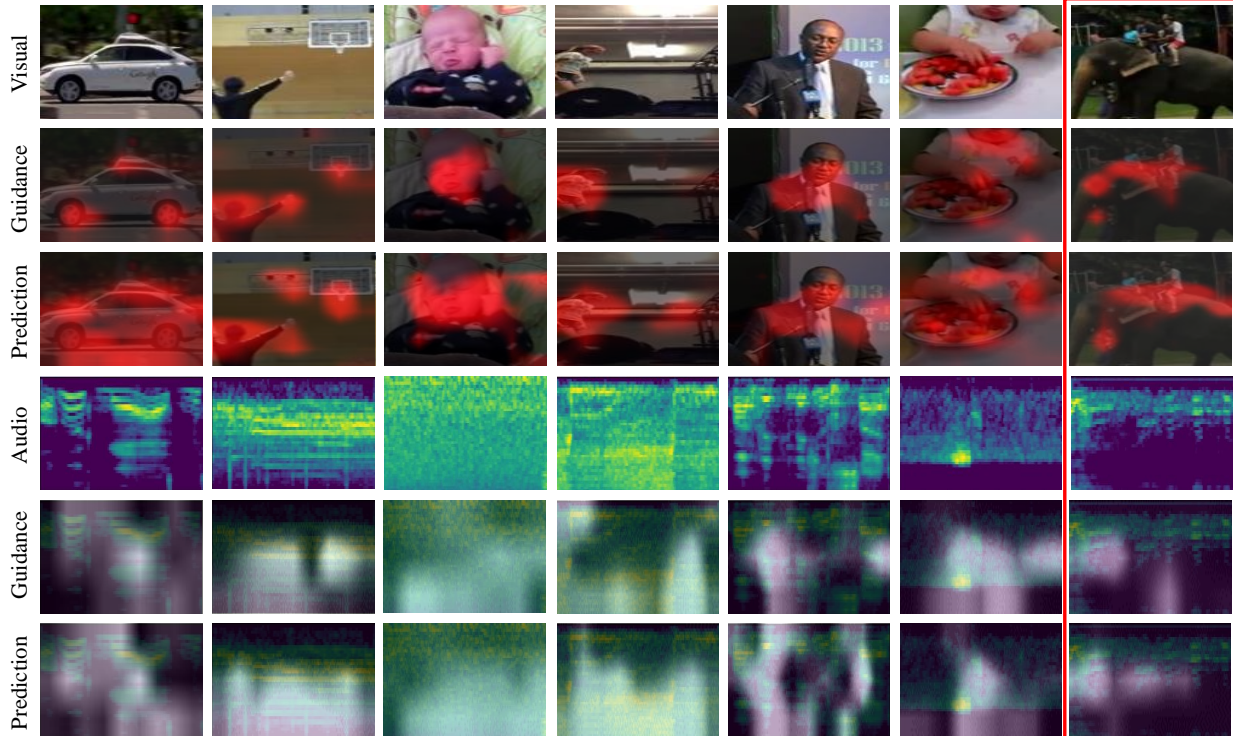


Figure 5. Visualization of attention maps generated from cross-modal filters (Guidance) and encoders (Prediction) for both visual and audio modalities. The last column is a bad case with messy background and interlaced objects, where the localized regions are not precise.

#### 4.3.4 Analysis of Within-modal Information in Contrastive Loss

Here we explore which kind of within-modal information really works in cross-modal contrastive learning. Two types of sampling policies are considered: a) Within-modal negative sampling that takes two samples (with same modality) from different videos to form a negative pair and distinguishes them as in Eq. (7); b) Within-modal positive sampling that takes two samples (with same modality) from the same video to form a positive pair and aligns them. Note that using both policies actually forms the strategy in AVID [30]. The results are shown in Table 3. We observe that the negative sampling could benefit CMAC a lot on both datasets without extra memory expense, since we can simply utilize the samples from previous batch (stored in memory bank) to form negative pairs. In contrast, the positive sampling harms the performance and even costs twice as much memory as negative sampling, due to that it requires saving two clips for each video. The possible reason for the performance drop is that aligning within-modal positive pairs would discard the intrinsic temporal synchronization in each video.

Both the within-modal information in contrastive loss and the proposed attention consistency mechanism make up the impressive results of CMAC. According to our observa-

Table 3. Effects of within-modal negative samples (w/i Neg) and within-modal positive samples (w/i Pos) in the contrastive loss of CMAC. Iter. indicates the iteration number required for an epoch.

	w/i Neg	w/i Pos	Iter.	UCF101	HMDB51
CMAC	✗	✗	3,509	86.5	57.0
	✓	✗	3,509	87.2	57.8
	✗	✓	7,018	86.2	56.4
	✓	✓	7,018	86.7	57.5

tion, both of them can bring considerable improvements, indicating that they are complementary.

#### 4.4. Visualization for Cross-modal Attention

The key insight of CMAC is that forcing the visual encoder  $f_v(\cdot)$  to attend to regions where sounds are made, and the audio encoder  $f_a(\cdot)$  to ground the frequencies belonging to the interested objects. Thus, we first visualize the attention maps generated from cross-modal filters in Fig. 5 (Guidance row). It can be observed that, taking the car image as an example, our audio-guided attention can successfully localize the car wheel regions where the wheel noises are made in the visual frames. As a contrast, the attended regions from  $f_v(\cdot)$  itself (Prediction row) focus on the whole car body, because  $f_v(\cdot)$  is more interested in global information without cross-modal local correspondence. It reveals that the visual guidance from audio signals could be an ef-

Table 4. Comparison of video action recognition on UCF-101 and HMDB-51, which are pretrained on Kinetics-400. Averaged top-1 accuracy across official splits is reported. Method with \* indicates that additional video texts (*e.g.* title) are used as supervision.

Methods	Backbone	Pretrained Dataset	Input Size	Batch Size	Epoch	UCF101	HMDB51
Multisensory[34]	3D-ResNet18	Kinetics-400	$64 \times 224^2$	64	400	82.1	-
CPD*[27]	3D-ResNet50	Kinetics-400	$8 \times 224^2$	128	110	88.7	57.7
AVTS[25]	MC3-18	Kinetics-400	$25 \times 224^2$	64	90	85.5	56.9
AV Sync+RotNet[49]	AVSlowFast	Kinetics-400	$64 \times 224^2$	1024	120	87.0	54.6
SpeedNet[5]	S3D	Kinetics-400	$16 \times 224^2$	-	81.1	48.8	-
XDC[1]	R(2+1)D-18	Kinetics-400	$32 \times 224^2$	32	120	86.8	52.6
AVID[30]	R(2+1)D-18	Kinetics-400	$32 \times 224^2$	256	400	87.5	60.8
GDT[38]	R(2+1)D-18	Kinetics-400	$32 \times 128^2$	768	200	89.3	60.0
CMAC	R(2+1)D-18	Kinetics-400	$32 \times 128^2$	128	200	<b>90.3</b>	<b>61.1</b>

Table 5. Comparison of full retrieval on UCF101 and HMDB51 datasets, which are pretrained on Kinetics-400.

Recall @	UCF101			HMDB51		
	1	5	10	1	5	10
ClipOrder[50]	14.1	30.3	40.4	7.6	22.9	34.4
SpeedNet[5]	13.0	28.1	37.5	-	-	-
VCP[28]	18.6	33.6	42.5	7.6	24.4	36.3
VSP[8]	24.6	41.9	51.3	10.3	26.6	38.8
GDT[38]	57.4	73.4	80.8	25.4	51.4	63.9
CMAC	<b>58.4</b>	<b>74.2</b>	<b>81.3</b>	<b>26.0</b>	<b>52.2</b>	<b>64.2</b>

fective supervision to constrain  $f_v(\cdot)$  to focus on local regions with sounds, which brings significant improvements as shown in Table 1. In terms of audio encoder  $f_a(\cdot)$ , the localized frequencies with guidance from visual signals are more sparse than the focused frequencies from  $f_a(\cdot)$  itself.

However, CMAC is not always effective in localizing correct visual and audio local regions, as shown in the last column of Fig. 5. When the video has the messy background and interlaced objects, it is hard to precisely match the corresponding local patterns without human annotations. Nevertheless, these observations prove that the cross-modal attention consistency is intuitive and reasonable in visual-audio unsupervised representation learning.

#### 4.5. Comparison with State-of-the-arts

Given our best setting, we train CMAC with longer epochs of 200 and strong color jitter augmentation in [38], and transfer the pretrained representations to various downstream tasks.

**Video Recognition.** We evaluate CMAC on two video action recognition benchmarks of UCF101 and HMDB51. The results are reported in Table 4, which shows that CMAC obtains impressive results on both UCF101 and HMDB51. It should be noted that CMAC is a computation-friendly method. Particularly, GDT [38] utilizes 6 times of GPU cost and batch size than CMAC, while CMAC surpasses GDT about 1.0% on UCF101 and 1.1% on HMDB51. Compared to AVID [30], CMAC also adopts much smaller batch size and fewer epochs to obtain 2.8% improvement on UCF101 and 0.3% on HMDB51. The results reveal that the bidirectional local correspondence is effective in boosting the visual representation learning. After teaching the visual en-

Table 6. Comparison of audio classification by quickly training a linear classifier. The pretrained dataset is Kinetics-400.

Methods	ESC50	Methods	D2013	D2014
SoundNet[4]	74.2	Scratch	48	-
AVTS[25]	76.7	Single-Modal	61	-
AVID[30]	79.1	Baseline	68	89
XDC*[1]	78.0	AVTS[30]	-	91
GDT[38]	78.6	GDT[38]	73	94
CMAC	<b>81.4</b>	CMAC	<b>76</b>	<b>96</b>

(a) \* indicates that the backbone encoder  $f_a(\cdot)$  is also finetuned on ESC50.

(b) The baseline is a general cross-modal contrastive loss as defined in Eq. (2).

coder where to focus on, it becomes easier to understand the visual content and distinguish different video instances. Thus, CMAC requires fewer batch size and epoch to surpass most of the existing methods.

**Video Retrieval.** For video retrieval, we evaluate the pretrained representations from CMAC on UCF101 and HMDB51 without finetuning the backbone. The results are given in Table 5, from which we observe that CMAC achieves new state-of-the-art performance in all settings. This shows that video representations of similar object content from CMAC become closer than those from previous methods, because the attention consistency makes the visual encoder focus on the correct object regions.

**Audio Classification.** For the audio classification task, we evaluate the pretrained model from CMAC on ESC50, DCASE2013, and DCASE2014 benchmarks. Notably, the reported results of compared methods are pretrained on Kinetic-400. Table 6 demonstrates that the pretrained model from CMAC outperforms existing methods by a large margin, *e.g.* 2.8% improvement on ESC50. Note that XDC further finetunes the backbone  $f_a(\cdot)$  on the downstream task, while CMAC only learns the classifier and obtains better performance. For DCASE2013 and DCASE2014, the result of GDT is obtained by using their official model pretrained on Kinetics-400. The superiority attributes to the localized voice frequencies according to target objects, which also proves the effectiveness of the proposed CMAC.



## 5. Conclusion

In this paper, we propose a novel pretext task for visual-audio unsupervised representation learning, namely Cross-Modal Attention Consistency (CMAC). The core insight of CMAC is that the visual perception encoder should attention to regions where sounds are made, and the auditory perception should ground acoustic-frequencies of sounding objects, which we call bidirectional local correspondence. To model such a bidirectional local correspondence supervision, CMAC aims to align the regional attention maps purely from visual signals with the target attention guidance from audio signals, and vice versa. Accompanied by a remoulded cross-modal contrastive loss with additional within-modal interactions, CMAC obtains impressive results on various downstream tasks.

## References

- [1] Humam Alwassel, Dhruv Mahajan, Lorenzo Torresani, Bernard Ghanem, and Du Tran. Self-supervised learning by cross-modal audio-video clustering. *Advances in Neural Information Processing Systems*, 33, 2020.
- [2] Relja Arandjelovic and Andrew Zisserman. Look, listen and learn. In *Proceedings of the IEEE International Conference on Computer Vision*, pages 609–617, 2017.
- [3] Relja Arandjelovic and Andrew Zisserman. Objects that sound. In *Proceedings of the European Conference on Computer Vision (ECCV)*, pages 435–451, 2018.
- [4] Yusuf Aytar, Carl Vondrick, and Antonio Torralba. Soundnet: Learning sound representations from unlabeled video. In *Advances in neural information processing systems*, pages 892–900, 2016.
- [5] Sagie Benaim, Ariel Ephrat, Oran Lang, Inbar Mosseri, William T Freeman, Michael Rubinstein, Michal Irani, and Tali Dekel. Speednet: Learning the speediness in videos. In *Proceedings of the IEEE/CVF Conference on Computer Vision and Pattern Recognition*, pages 9922–9931, 2020.
- [6] Mathilde Caron, Ishan Misra, Julien Mairal, Priya Goyal, Piotr Bojanowski, and Armand Joulin. Unsupervised learning of visual features by contrasting cluster assignments. *Advances in neural information processing systems*, 2020.
- [7] Ting Chen, Simon Kornblith, Mohammad Norouzi, and Geoffrey Hinton. A simple framework for contrastive learning of visual representations. *arXiv preprint arXiv:2002.05709*, 2020.
- [8] Hyeon Cho, Taehoon Kim, Hyung Jin Chang, and Wonjun Hwang. Self-supervised spatio-temporal representation learning using variable playback speed prediction. *arXiv preprint arXiv:2003.02692*, 2020.
- [9] Virginia R de Sa. Learning classification with unlabeled data. In *Advances in neural information processing systems*, pages 112–119, 1994.
- [10] Carl Doersch, Abhinav Gupta, and Alexei A Efros. Unsupervised visual representation learning by context prediction. In *Proceedings of the IEEE international conference on computer vision*, pages 1422–1430, 2015.
- [11] Alexey Dosovitskiy, Jost Tobias Springenberg, Martin Riedmiller, and Thomas Brox. Discriminative unsupervised feature learning with convolutional neural networks. In *Advances in neural information processing systems*, pages 766–774, 2014.
- [12] Ruohan Gao, Rogerio Feris, and Kristen Grauman. Learning to separate object sounds by watching unlabeled video. In *Proceedings of the European Conference on Computer Vision (ECCV)*, pages 35–53, 2018.
- [13] Ruohan Gao and Kristen Grauman. Co-separating sounds of visual objects. In *Proceedings of the IEEE International Conference on Computer Vision*, pages 3879–3888, 2019.
- [14] Jort F Gemmeke, Daniel PW Ellis, Dylan Freedman, Aren Jansen, Wade Lawrence, R Channing Moore, Manoj Plakal, and Marvin Ritter. Audio set: An ontology and human-labeled dataset for audio events. In *2017 IEEE International Conference on Acoustics, Speech and Signal Processing (ICASSP)*, pages 776–780. IEEE, 2017.
- [15] Spyros Gidaris, Praveer Singh, and Nikos Komodakis. Unsupervised representation learning by predicting image rotations. *arXiv preprint arXiv:1803.07728*, 2018.
- [16] Jean-Bastien Grill, Florian Strub, Florent Altché, Corentin Tallec, Pierre H Richemond, Elena Buchatskaya, Carl Doersch, Bernardo Avila Pires, Zhaohan Daniel Guo, Mohammad Gheshlaghi Azar, et al. Bootstrap your own latent: A new approach to self-supervised learning. *arXiv preprint arXiv:2006.07733*, 2020.
- [17] Raia Hadsell, Sumit Chopra, and Yann LeCun. Dimensionality reduction by learning an invariant mapping. In *2006 IEEE Computer Society Conference on Computer Vision and Pattern Recognition*, volume 2, pages 1735–1742. IEEE, 2006.
- [18] David Harwath, Adria Recasens, Dídac Surís, Galen Chuang, Antonio Torralba, and James Glass. Jointly discovering visual objects and spoken words from raw sensory input. In *Proceedings of the European conference on computer vision (ECCV)*, pages 649–665, 2018.
- [19] Kaiming He, Haoqi Fan, Yuxin Wu, Saining Xie, and Ross Girshick. Momentum contrast for unsupervised visual representation learning. In *Proceedings of the IEEE/CVF Conference on Computer Vision and Pattern Recognition*, pages 9729–9738, 2020.
- [20] Kaiming He, Xiangyu Zhang, Shaoqing Ren, and Jian Sun. Deep residual learning for image recognition. In *Proceedings of the IEEE conference on computer vision and pattern recognition*, pages 770–778, 2016.
- [21] Olivier J Hénaff, Aravind Srinivas, Jeffrey De Fauw, Ali Razavi, Carl Doersch, SM Eslami, and Aaron van den Oord. Data-efficient image recognition with contrastive predictive coding. *arXiv preprint arXiv:1905.09272*, 2019.
- [22] R Devon Hjelm, Alex Fedorov, Samuel Lavoie-Marchildon, Karan Grewal, Phil Bachman, Adam Trischler, and Yoshua Bengio. Learning deep representations by mutual information estimation and maximization. *arXiv preprint arXiv:1808.06670*, 2018.
- [23] Di Hu, Feiping Nie, and Xuelong Li. Deep multimodal clustering for unsupervised audiovisual learning. In *Proceedings of the IEEE/CVF Conference on Computer Vision and Pattern Recognition*, pages 9248–9257, 2019.

- [24] Will Kay, Joao Carreira, Karen Simonyan, Brian Zhang, Chloe Hillier, Sudheendra Vijayanarasimhan, Fabio Viola, Tim Green, Trevor Back, Paul Natsev, et al. The kinetics human action video dataset. *arXiv preprint arXiv:1705.06950*, 2017.
- [25] Bruno Korbar, Du Tran, and Lorenzo Torresani. Cooperative learning of audio and video models from self-supervised synchronization. In *Advances in Neural Information Processing Systems*, pages 7763–7774, 2018.
- [26] Hildegard Kuehne, Hueihan Jhuang, Estíbaliz Garrote, Tomaso Poggio, and Thomas Serre. Hmdb: a large video database for human motion recognition. In *2011 International Conference on Computer Vision*, pages 2556–2563. IEEE, 2011.
- [27] Tianhao Li and Limin Wang. Learning spatiotemporal features via video and text pair discrimination. *arXiv preprint arXiv:2001.05691*, 2020.
- [28] Dezhao Luo, Chang Liu, Yu Zhou, Dongbao Yang, Can Ma, Qixiang Ye, and Weiping Wang. Video cloze procedure for self-supervised spatio-temporal learning. *arXiv preprint arXiv:2001.00294*, 2020.
- [29] Antoine Miech, Jean-Baptiste Alayrac, Lucas Smaira, Ivan Laptev, Josef Sivic, and Andrew Zisserman. End-to-end learning of visual representations from uncurated instructional videos. In *Proceedings of the IEEE/CVF Conference on Computer Vision and Pattern Recognition*, pages 9879–9889, 2020.
- [30] Pedro Morgado, Nuno Vasconcelos, and Ishan Misra. Audio-visual instance discrimination with cross-modal agreement. *arXiv preprint arXiv:2004.12943*, 2020.
- [31] Arsha Nagrani, Chen Sun, David Ross, Rahul Sukthankar, Cordelia Schmid, and Andrew Zisserman. Speech2action: Cross-modal supervision for action recognition. In *Proceedings of the IEEE/CVF Conference on Computer Vision and Pattern Recognition*, pages 10317–10326, 2020.
- [32] Mehdi Noroozi and Paolo Favaro. Unsupervised learning of visual representations by solving jigsaw puzzles. In *European Conference on Computer Vision*, pages 69–84. Springer, 2016.
- [33] Aaron van den Oord, Yazhe Li, and Oriol Vinyals. Representation learning with contrastive predictive coding. *arXiv preprint arXiv:1807.03748*, 2018.
- [34] Andrew Owens and Alexei A Efros. Audio-visual scene analysis with self-supervised multisensory features. In *Proceedings of the European Conference on Computer Vision (ECCV)*, pages 631–648, 2018.
- [35] Andrew Owens, Jiajun Wu, Josh H McDermott, William T Freeman, and Antonio Torralba. Ambient sound provides supervision for visual learning. In *European conference on computer vision*, pages 801–816. Springer, 2016.
- [36] Daniel S Park, William Chan, Yu Zhang, Chung-Cheng Chiu, Barret Zoph, Ekin D Cubuk, and Quoc V Le. Specaugment: A simple data augmentation method for automatic speech recognition. *arXiv preprint arXiv:1904.08779*, 2019.
- [37] Deepak Pathak, Ross Girshick, Piotr Dollár, Trevor Darrell, and Bharath Hariharan. Learning features by watching objects move. In *Proceedings of the IEEE Conference on Computer Vision and Pattern Recognition*, pages 2701–2710, 2017.
- [38] Mandela Patrick, Yuki M Asano, Ruth Fong, João F Henriques, Geoffrey Zweig, and Andrea Vedaldi. Multi-modal self-supervision from generalized data transformations. *arXiv preprint arXiv:2003.04298*, 2020.
- [39] Karol J Piczak. Esc: Dataset for environmental sound classification. In *Proceedings of the 23rd ACM international conference on Multimedia*, pages 1015–1018, 2015.
- [40] AJ Piergiovanni, Anelia Angelova, and Michael S Ryoo. Evolving losses for unsupervised video representation learning. In *Proceedings of the IEEE/CVF Conference on Computer Vision and Pattern Recognition*, pages 133–142, 2020.
- [41] Andrew Rouditchenko, Hang Zhao, Chuang Gan, Josh McDermott, and Antonio Torralba. Self-supervised audio-visual co-segmentation. In *ICASSP 2019-2019 IEEE International Conference on Acoustics, Speech and Signal Processing (ICASSP)*, pages 2357–2361. IEEE, 2019.
- [42] Arda Senocak, Tae-Hyun Oh, Junsik Kim, Ming-Hsuan Yang, and In So Kweon. Learning to localize sound source in visual scenes. In *Proceedings of the IEEE Conference on Computer Vision and Pattern Recognition*, pages 4358–4366, 2018.
- [43] Khurram Soomro, Amir Roshan Zamir, and Mubarak Shah. Ucf101: A dataset of 101 human actions classes from videos in the wild. *arXiv preprint arXiv:1212.0402*, 2012.
- [44] Dan Stowell, Dimitrios Giannoulis, Emmanouil Benetos, Mathieu Lagrange, and Mark D Plumbley. Detection and classification of acoustic scenes and events. *IEEE Transactions on Multimedia*, 17(10):1733–1746, 2015.
- [45] Chen Sun, Austin Myers, Carl Vondrick, Kevin Murphy, and Cordelia Schmid. Videobert: A joint model for video and language representation learning. In *Proceedings of the IEEE International Conference on Computer Vision*, pages 7464–7473, 2019.
- [46] Du Tran, Heng Wang, Lorenzo Torresani, Jamie Ray, Yann LeCun, and Manohar Paluri. A closer look at spatiotemporal convolutions for action recognition. In *Proceedings of the IEEE conference on Computer Vision and Pattern Recognition*, pages 6450–6459, 2018.
- [47] Xiaolong Wang and Abhinav Gupta. Unsupervised learning of visual representations using videos. In *Proceedings of the IEEE international conference on computer vision*, pages 2794–2802, 2015.
- [48] Zhirong Wu, Yuanjun Xiong, Stella X Yu, and Dahua Lin. Unsupervised feature learning via non-parametric instance discrimination. In *Proceedings of the IEEE Conference on Computer Vision and Pattern Recognition*, pages 3733–3742, 2018.
- [49] Fanyi Xiao, Yong Jae Lee, Kristen Grauman, Jitendra Malik, and Christoph Feichtenhofer. Audiovisual slowfast networks for video recognition. *arXiv preprint arXiv:2001.08740*, 2020.
- [50] Dejing Xu, Jun Xiao, Zhou Zhao, Jian Shao, Di Xie, and Yueting Zhuang. Self-supervised spatiotemporal learning via video clip order prediction. In *Proceedings of the IEEE Conference on Computer Vision and Pattern Recognition*, pages 10334–10343, 2019.

- [51] Hang Zhao, Chuang Gan, Andrew Rouditchenko, Carl Vondrick, Josh McDermott, and Antonio Torralba. The sound of pixels. In *Proceedings of the European conference on computer vision (ECCV)*, pages 570–586, 2018.
- [52] Chengxu Zhuang, Alex Lin Zhai, and Daniel Yamins. Local aggregation for unsupervised learning of visual embeddings. In *Proceedings of the IEEE International Conference on Computer Vision*, pages 6002–6012, 2019.